Available online at www.sciencedirect.com
ScienceDirect
Journal of Solid State Chemistry 180 (2007) 1967–1976
JOURNAL OF SOLID STATE CHEMISTRY
www.elsevier.com/locate/jssc

Evidences for decarbonation and exfoliation of layered double hydroxide in *N*,*N*-dimethylformamide–ethanol solvent mixture

Claudia R. Gordijo, Vera R. Leopoldo Constantino, Denise de Oliveira Silva*

Departamento de Química Fundamental, Instituto de Química, Universidade de São Paulo, CP 26077, CEP 05513-900, São Paulo, SP, Brazil

Received 5 January 2007; received in revised form 4 May 2007; accepted 6 May 2007
Available online 13 May 2007

Abstract

The behavior of a Hydrotalcite-like material (carbonate-containing Mg,Al-layered double hydroxide) in *N*,*N*-dimethylformamide (DMF)–ethanol mixture, at ambient temperature, has been investigated. The releasing of CO_2 and production of a formate-containing material occurred mainly for 1:1 (v/v) solvent mixture. Decarbonation of Hydrotalcite is promoted by DMF hydrolysis followed by neutralization of brucite-like layers through $HCOO^-$ intercalation. Translucent colloidal dispersion of LDH nanoparticles from the formate-containing phase was characterized by transmission electron (TEM) and atomic force (AFM) microscopies. The absence of (00ℓ) reflection at X-ray diffraction (XRD) pattern for dried colloidal dispersion indicated delamination of Hydrotalcite. The restacked sample exhibited broad reflections and typical hydroxide ordered layers non-basal (110) diffraction peaks. A LDH-$HCOO^-$ material was also prepared and characterized by FTIR and FT-Raman spectroscopies. Decarbonation and exfoliation of Hydrotalcite in *N*,*N*-dimethylformamide–ethanol mixed solvent provide an interesting method for preparation of new intercalated LDH materials.

Keywords: Layered double hydroxide; Anionic clays; Hydrotalcite; Exfoliation; Delamination; Formate intercalation

1. Introduction

Exfoliation or delamination of layered compounds is a very important process in the fields of materials chemistry and nanotechnology. It is also a useful method to prepare advanced two-dimensional functional materials. Dispersions of exfoliated lamellar compounds have been used for intercalation of bulky (bio)molecules; production of high specific area heterogeneous catalysts; multilayer thin films for sensors, electrodes, coatings and membranes; hollow nanotubes, nanorods and nanowires by soft chemical route; polymer–inorganic nanocomposites and interstratificated materials [1–3].

The spontaneous exfoliation of minerals such as smectite clays in water gives aluminosilicate nanosheets. In contrast, the delamination of high layer charge density materials to give nanometer thickness particles can be achieved only after interlayer modification [1]. Appropriate combination of interlamellar ion and solvent, for example, can be used to promote exfoliation of two-dimensionally (2D) ordered structures such as metal phosphates [4], transition-metal dichalcogenides [5], titanates [6], niobates [7] and molybdic acid [8]. The majority of delaminated layered systems produce colloidal dispersions of negatively charged inorganic nanoparticles and, therefore, the study of layered double hydroxides (LDHs) is very interesting since they are able to generate complementary new materials by giving positively charged nanosheets [9].

The structure of LDHs is based on octahedral brucite-(magnesium hydroxide-) like layers, where some divalent cations have been replaced by trivalent ions giving positively charged layers that are compensated by the presence of intercalated anions [10]. The typical LDH formula is $[M^{II}_{1-x}M^{III}_x(OH)_2]^{x+}(A^{n-})_{x/n}\cdot yH_2O$, where M^{II} and M^{III} represent divalent (Mg^{2+}, Zn^{2+}, Co^{2+}, etc.) and trivalent (Al^{3+}, Cr^{3+}, Fe^{3+}, etc.) cations, respectively; A^{n-} is a *n*-valent anion; and yH_2O indicates the interlayer water molecules. This type of structure can support several divalent and trivalent cations and a range of interlayer

*Corresponding author. Fax: +55 11 38155579.
E-mail address: deosilva@iq.usp.br (D. de Oliveira Silva).

0022-4596/$ - see front matter © 2007 Elsevier Inc. All rights reserved.
doi:10.1016/j.jssc.2007.05.003

anions, carbonate being the most common charge-balancing anion [11]. The structural versatility allows the isolation of LDHs with wide-ranging functionalities and applications or potential as catalysts [10,12], support for catalysts [13,14], reinforced fillers for synthetic or natural organic polymers [15,16], ion-exchangers for environmental remediation [17], and components for pharmaceutical and cosmetics formulations [18,19]. These anionic two-dimensional materials have also been named "Hydrotalcite-like" compounds in reference to the structural resemblance with the mineral Hydrotalcite, a magnesium–aluminum LDH of composition $[Mg_6Al_2(OH)_{16}](CO_3)\cdot 4H_2O$.

LDH materials have high layer charge density (i.e., strong interlayer electrostatic interactions in a small area) and, consequently, exfoliation processes have been achieved only under specific conditions. The delamination of LDHs was firstly observed by modifying the interlayer region with intercalated anionic long carbon chain organic species. LDHs containing surfactants (such as dodecylsulfate) have been successfully delaminated in solvents like alcohols (butanol, pentanol, hexanol, octanol, etc.) [20–23], acrylate monomers (such as 2-hydroxyethyl methacrylate) [24], formamide [25] and tetrachlorocarbon [26]. The influences of M^{II}/M^{III} molar ratio, nature of cations, intercalated surfactant anion and organic solvent on exfoliation of LDHs have also been described [27].

Studies have reported that the use of formamide ($HCONH_2$) as solvent leads to clear colloidal dispersions of glycine-containing Mg,Al-LDH [28] and other amino acids-containing M^{II},Al-LDH (M^{II} = Mg, Ni, Co or Zn) [29]. The delamination of LDHs intercalated by small inorganic anions such as nitrate [30,31], chloride and perchlorate [32,33] can also be achieved in formamide suspensions. The exfoliation of LDHs in the formamide solvent and its possible applications has been recently reviewed [34]. Delamination of LDHs layers has also been reached in water solvent for lactate-containing Mg,Al-LDH [35] and Zn,Al-LDH [36]. The use of water is very interesting to intercalate attractive polar (bio)molecules. In addition, some of the reports mentioned above have described the restacking of LDH solvated monolayers by evaporating the solvent or changing the polarity of the medium.

Possible applications of these exfoliated LDH nanosheets are highlighted in the literature, for example, as composite films with anionic polymer [32], highly oriented thin films [33], nanocomposites with neutral synthetic organic polymers [9,37,38], quantum dot composites [39] and building blocks for preparation of hollow spheres [40].

In spite of all these important applications, the LDHs exfoliation processes still deserve more attention. Some of the systems described above require heat treatment to give colloidal dispersions while other ones must be ultrasound assisted. All the previously reported exfoliation strategies are mainly related to interactions or miscibility of the solvents with the interlayer species involving London forces or hydrogen bonds. Furthermore, direct exfoliation of Hydrotalcite is challenging because the high affinity of carbonate anions for LDH layers precludes direct anion exchange reaction and exfoliation.

In the present paper, the exfoliation of the carbonate-containing LDH was achieved by a simple procedure. Hydrotalcite was suspended in *N*,*N*-dimethylformamide (DMF)–ethanol mixed solvent at ambient temperature. The LDH exfoliated phase (containing formate as charge balancing ions) was obtained through Hydrotalcite decarbonation promoted by the solvent hydrolysis. A LDH-formate (LDH-$HCOO^-$) material has also been prepared to help the characterization of the formate-containing phase in the delaminated material.

2. Experimental section

2.1. Materials

All reagents were of analytical grade and used as received, without further purification: $Mg(NO_3)_2\cdot 6H_2O$, $Al(NO_3)_3\cdot 9H_2O$, Na_2CO_3, NaOH, HCl solution, DMF and ethanol (all from Merck), formic acid (Synth), sodium formate (Vetec).

2.2. Synthesis of Hydrotalcite (LDH-carbonate)

LDH-carbonate with Mg^{2+}/Al^{3+} molar ratio of three was prepared by co-precipitation procedure [41]. A mixed aqueous solution (ca. 240 mL) containing $Mg(NO_3)_2\cdot 6H_2O$ (23.07 g, 89.7 mmol) and $Al(NO_3)_3\cdot 9H_2O$ (11.25 g, 29.9 mmol,) was slowly added dropwise into deionized water (ca. 100 mL) under stirring. The pH was kept approximately constant at 10 by continuously adding 0.1 mol/L Na_2CO_3 solution followed by addition of a 2 mol/L NaOH aqueous solution. The resulting suspension was stirred for 12 h, at 80 °C. The solid was isolated by centrifugation, washed with 0.1 mol/L Na_2CO_3 solution and, then, thoroughly washed with water, and dried at 80 °C for 48 h. Anal. Calc. for LDH-carbonate of composition $[Mg_3Al(OH)_8](CO_3)_{0.5}\cdot 3.0\ H_2O$: C: 1.9%; H: 4.4%, Mg: 22.8%; Al: 8.4%; Mg/Al = 3.0; found C: 2.3%; H: 3.7%, Mg: 22.1%; Al: 7.8%; Mg/Al = 3.1. Content of water, 17.6% (w/w), was determined by thermogravimetric analysis as described before [19]. FTIR bands/cm^{-1} at: 3500 (νOH, stretching vibrations of hydroxyl groups of brucite-like layers and water molecules); 3050 ($\nu OH\ldots CO_3^{2-}$, OH stretching of water molecules forming hydrogen bonds with carbonate ions); 1646 (δH_2O, angular deformation of water); 1373 (ν_3 CO_3^{2-}, stretching vibration of intercalated carbonate) and 663 (*M*–O vibrations) [42]. X-ray diffraction (XRD) peaks at 2θ/degrees (d_{hkl}/nm): 11.32 (d_{003} = 0.781); 22.78 (d_{006} = 0.391); 34.57 (d_{012} = 0.259); 38.96 (d_{015} = 0.231); 46.08 (d_{018} = 0.197); 60.40 (d_{110} = 0.153) and 61.66 (d_{113} = 0.150) [11]. This LDH-carbonate with Mg^{2+}/Al^{3+} molar ratio of three was used for LDH exfoliation and formate intercalation experiments.

2.3. Isolation of LDH-samples from DMF–ethanol solvent mixtures

Amounts of 0.15 g of the LDH-carbonate were separately suspended in ca. 75 mL of DMF–ethanol mixtures according to the following DMF:ethanol proportions (v/v): 1:0 (i.e., 100% DMF; *LDH-sample A*); 3:1 (i.e., 75% DMF: 25% ethanol; *LDH-sample B*); 1:1 (i.e., 50% DMF : 50% ethanol; *LDH-sample C*); 1:3 (i.e., 25% DMF: 75% ethanol; *LDH-sample D*); 0:1 (i.e., 100% ethanol; *LDH-sample E*). All the suspensions were maintained in sealed flasks under mechanical shaking for 1 week, at ambient temperature. LDH-samples were isolated by centrifugation, washed with deionized water and ethanol, and then dried *in vacuum*. Anal. found for *LDH-sample C*: C: 3.9%; H: 3.5%, Mg: 19.2%; Al: 7.8%; Mg/Al = 2.7.

2.4. Detection of CO_2 and determination of carbonate loss percentage

The procedure described in Section 2.3 was repeated for all the five LDH-samples (A–E), but the sealed reaction flasks were now connected to flasks containing $Ba(OH)_2$ saturated aqueous solutions. After 1 week, white precipitates of $BaCO_3$ had appeared in the barium solutions indicating the release of CO_2 from the pristine LDH-carbonate for all the samples. The percentages of carbonate loss were determined in another experiment by monitoring the pH changes of the samples in aqueous suspensions with addition of HCl solution. In a typical procedure, 0.1 mol/L HCl solution was added stepwise to 100 mg of each solid sample suspended in 10 mL of deionized water, under magnetic stirring, at about 35 °C, up to 50 mL of added HCl (pH reached the value of ca. 1). The pH values were plotted as a function of the HCl added volumes for all LDH-samples as previously described [19]. Each 100 mg of LDH carbonate required 25 mL of HCl solution to totally eliminate the carbonate ions. The percentages of carbonate loss were estimated by comparing the results for all LDH-samples with that of Hydrotalcite, which was assumed to contain 100% of carbonate.

2.5. Decarbonation and exfoliation of Hydrotalcite

The LDH-carbonate (0.150 g) prepared as described in Section 2.2 was suspended in ca. 75 mL of a mixture of 1:1 (v/v) DMF–ethanol in a sealed flask and maintained under magnetic stirring for 1 week. After that, the system was allowed to stand at ambient temperature for 2 weeks and then two phases were observed: (a) colloidal dispersion, and (b) sediment. The supernatant colloidal dispersion, collected by pipetting off, was used for XRD, transmission electron microscopy (TEM), atomic force microscopy (AFM) and FT-Raman studies.

2.6. Restacking of LDH layers

The colloidal dispersion obtained as described in Section 2.5 was rotoevaporated to eliminate all the solvent mixture, giving a solid residue of restacked LDH.

2.7. Synthesis of LDH-formate material

LDH-formate was prepared by re-precipitation by modifying a reported procedure [43]. A 0.1 mol/L formic acid aqueous solution (ca. 250 mL) was added to 0.30 g of LDH-carbonate under magnetic stirring, at 50 °C, dissolving the solid completely. This solution was slowly added dropwise and under magnetic stirring to an alkaline solution (ca. 100 mL of deionized water with the pH elevated to 10 by addition of 0.1 mol/L NaOH). The pH was maintained at about 9 by simultaneous slow addition of 0.1 mol/L NaOH. The resulting aqueous suspension containing a white precipitate was refluxed for 2 h. The solid was isolated by centrifugation, washed with deionized water and then dried *in vacuum*. Anal. found for *LDH-formate*: C: 3.8%; H: 3.7%, Mg: 15.6%; Al: 8.1%; Mg/Al = 2.1.

2.8. Characterization

Elemental chemical analyses (C, H and N) were carried out in a Perkin Elmer Elemental Analyzer, CHN 2000, at *Instituto de Química* (USP). Metals (Mg and Al) contents were determined in duplicate by ICP emission spectroscopy using a Spectro Analytical Instrument after dissolving the samples in 1% (v/v) nitric acid solutions. X-ray diffraction (XRD) patterns were recorded on a Rigaku diffractometer, Miniflex, using Cu Kα radiation (1.541 Å), 30 kV, 15 mA and step of 0.02°. The colloidal dispersion was directly dropped on a quartz plate and air-dried to give a film while powder samples were suspended in ethanol to give films. Fourier-Transform Infrared (FTIR) spectra of samples dispersed in KBr were recorded in the 4000–400 cm^{-1} region on a Bomen, MB-102, equipment coupled to a diffuse reflectance accessory (Pike Technologies, Inc.). Fourier-Transform Raman spectra (FT-Raman) of solid samples were recorded on a RFS 10 FT-Raman Bruker spectrometer (Nd-YAG laser, line 1064 nm). Scanning electron micrographs (SEM) of solids directly deposited in aluminum support were obtained using a JOEL JSM 840A electron microscope (accelerating voltage of 25 kV). Transmission electron microscope (TEM) images were performed on a Philips CM-200 microscope at 200 kV. The colloidal dispersion was dropped on a copper grid and it was covered with carbon film. Magnetic Alternated Current Atomic Force Microscopy, AFM-MAC MODE images were obtained on a PicoSPM I Molecular Imaging, under nitrogen atmosphere, at ambient temperature after the colloidal dispersion was air-dried on mica substrate.

3. Results and discussion

3.1. Decarbonation and exfoliation of Hydrotalcite

The Hydrotalcite (LDH-carbonate) prepared here by co-precipitation exhibited typical XRD pattern and FTIR profile of a well-crystallized LDH structure (as discussed later).

In a preliminary work conducted in our laboratory, we observed that Hydrotalcite suspended in some solvent mixtures of DMF–ethanol could give translucent colloidal dispersions. In order to elucidate this behavior, five distinct proportions of amide–alcohol (i.e., 1:0; 3:1; 1:1; 1:3 and 0:1 (v/v)) were investigated giving solid samples (respectively, LDH-samples A,B,C, D and E) from the pristine LDH-carbonate. The releasing of gas observed for certain of those solvent mixtures indicated the possible loss of carbonate anions (as carbon dioxide) from the LDH interlayers. The evolution of CO_2 was confirmed by collecting the precipitate formed into the $Ba(OH)_2$ solutions attached to the reaction flasks. The collected white solid was identified as barium carbonate ($BaCO_3$) showing a witherite typical XRD pattern (main *d*-spacing values/nm = 0.456; 0.373 ($I/I_{100} = 100\%$); 0.332; 0.264; 0.228; 0.215; 0.211; 0.204; 0.203; 0.194; 0.186; 0.167; 0.165; 0.163; 0.156; 0.152; 0.137) [44]. Visually it was possible to infer that the CO_2 released amount depends on the DMF–ethanol proportion, being LDH-sample A < LDH-sample-B < LDH-sample C > LDH-sample D > LDH-sample E. The estimated carbonate loss percentages (Fig. 1) confirm that the highest amount of $BaCO_3$ is formed when the solvents are equally mixed (1:1 DMF–ethanol).

Based on these results we can conclude that: (a) Hydrotalcite undergoes decarbonation when suspended in DMF; (b) the presence of ethanol seems to enhance the decarbonation process; (c) decarbonation is more pronounced when DMF and ethanol are mixed in equal amounts (i.e., 1:1 (v/v) proportion).

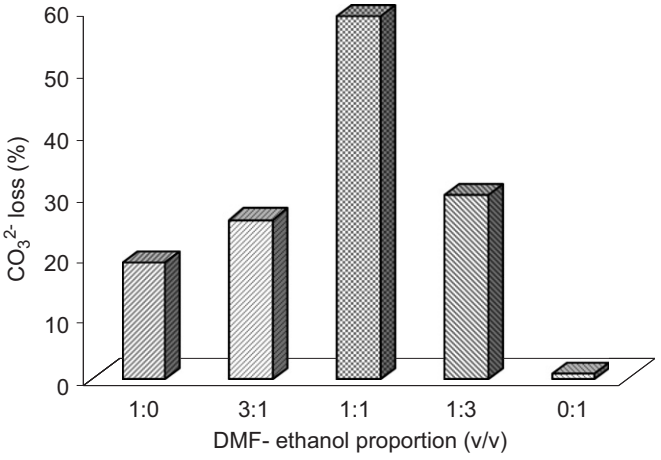

Fig. 1. Percentage of carbonate loss in function of the DMF:ethanol proportions (v/v) in the solvent mixtures.

In addition to decarbonation process, the treatment of LDH-carbonate with DMF–ethanol mixed solvent resulted in colloidal-aspect samples. The morphologies of LDH-carbonate and LDH-sample C particles were examined by SEM. The images (Fig. 2) show that the pristine LDH changed from the characteristic layered plate-like to a sheet-like morphology after treatment with 1:1 DMF–ethanol mixed solvent. Furthermore, some particles of LDH-sample C show wavy or flexible feature. The SEM studies, therefore, indicate delamination of Hydrotalcite in this mixture of solvents.

Taking into account the evidences for decarbonation and exfoliation of Hydrotalcite, another experimental procedure was conducted under similar conditions used to isolate LDH-sample C. However, instead of isolating all solid by centrifugation, the system was allowed to stand at ambient temperature for 2 weeks. Then, two phases were observed: a sediment (at the bottom) and a stable colloidal dispersion (at the top of the flask). The colloidal aspect of the upper phase was confirmed by Tyndall light scattering effect observed by a side incident light beam on the colloidal dispersion as shown in Fig. 3.

Restacking of the LDH layers was achieved by eliminating the solvents from the colloidal dispersion by rotoevaporation. The oriented film XRD patterns for pristine LDH-carbonate, colloidal dispersion, dried

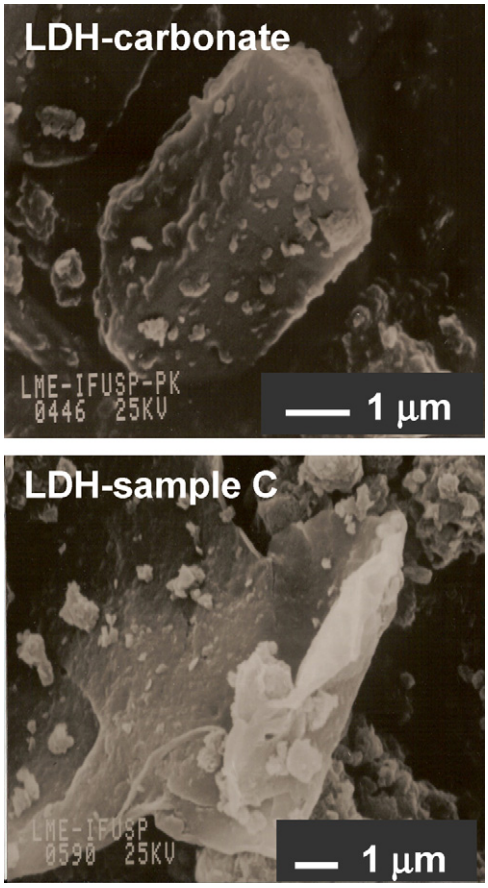

Fig. 2. SEM images of Hydrotalcite and LDH-sample C.

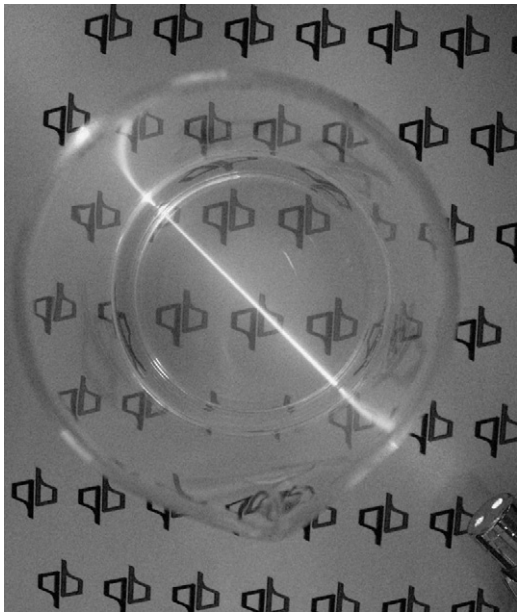

Fig. 3. Photograph of Hydrotalcite colloidal dispersion obtained from 1:1 (v/v) DMF–ethanol solvent mixture. The light beam incident from the side demonstrates the Tyndall effect.

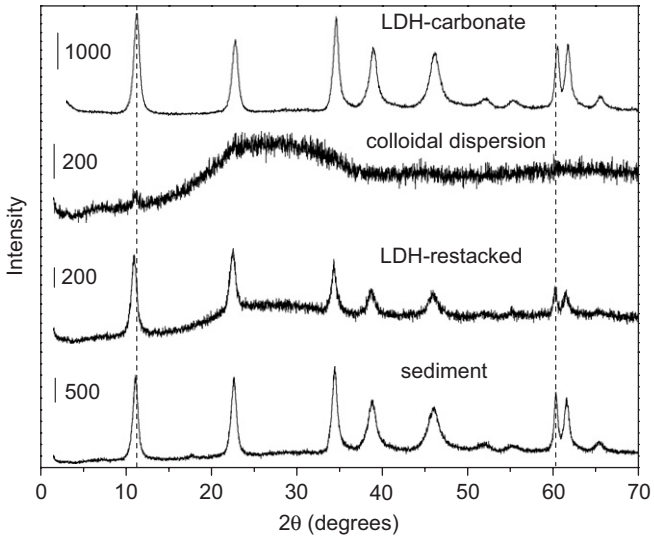

Fig. 4. XRD patterns of oriented films: pristine LDH-carbonate; colloidal dispersion; solid isolated after drying the colloidal dispersion; sediment recovered from the bottom during standing.

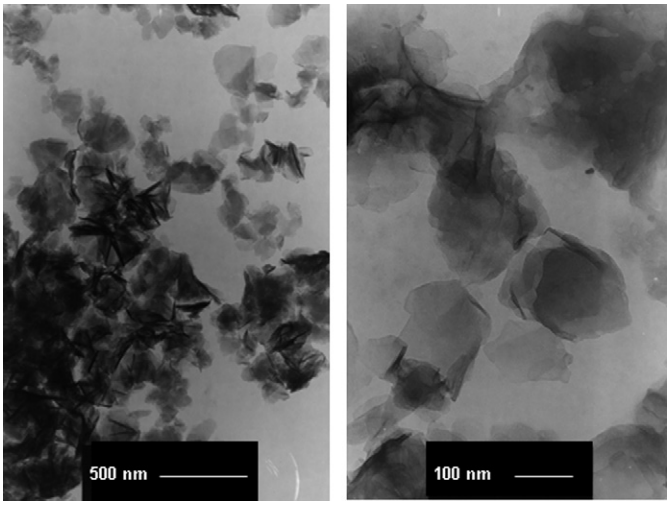

Fig. 5. TEM images of the colloidal dispersion.

colloidal dispersion solid and recovered sediment are shown in Fig. 4. The LDH-carbonate reflections can be indexed for a hexagonal lattice with *R3* m rhombohedral symmetry, which is commonly used for description of LDH structures [11]. The first diffraction peak ($2\theta = 11.32^{\circ}$) indexed to the 0 0 3 plane corresponds to a basal spacing (d_{003}) of about 0.78 nm, indicating isolation of LDH-carbonate with no impurities (indexation is reported in the Experimental Section). After treatment with 1:1 DMF–ethanol solvent mixture, the crystalline aspect of Hydrotalcite is lost. The solid material isolated by drying the colloidal dispersion on a quartz slide exhibits a broad amorphous-like halo. The absence of sharp basal (00ℓ) peaks suggests that the parallel (or face to face) arrangement of the LDH layers has been lost. These results reinforce evidences for exfoliation of considerable amount of Hydrotalcite. The XRD pattern of the restacked solid is very similar to that of the crystalline LDH (Fig. 4) showing that the triple layer cell with rhombohedral symmetry is maintained after restacking. The reflections for restacked sample are broader than those observed for the pristine LDH-carbonate suggesting the presence of smaller particles in the former. Turbostratic disorder was discarded since XRD simulations studies have indicated that the (113) reflection is affected by this kind of structural disorder [45] but this is not the case here. The presence of ordered hydroxide layers typical non-basal (110) diffraction peak for the restacked sample indicates that the brucite-like layers are preserved in the exfoliation process. The absence of more diffraction peaks suggests that the experimental conditions established here are soft enough to avoid formation of other crystalline phases. The sediment consists of LDH-carbonate phase that did not undergo delamination as shown by the similarity of its XRD pattern with that of the starting LDH-carbonate.

The exfoliation of Hydrotalcite in 1:1 DMF–ethanol solvent mixture was further confirmed by TEM and AFM images of the colloidal dispersion. TEM images (Fig. 5) show the formation of very thin particles that are almost transparent to the microscope electron beam, suggesting the presence of a few brucite-like layers. The observation of flexible and curled at the edges particles corroborates the proposition for Hydrotalcite delamination in nanometer range since the curling of thick particles is a very difficult process.

The AFM images for LDH-carbonate and colloidal dispersion at comparable scales are shown in Fig. 6. The former contains large particles (medium size of approximately 650 nm × 700 nm) while the colloidal dispersion

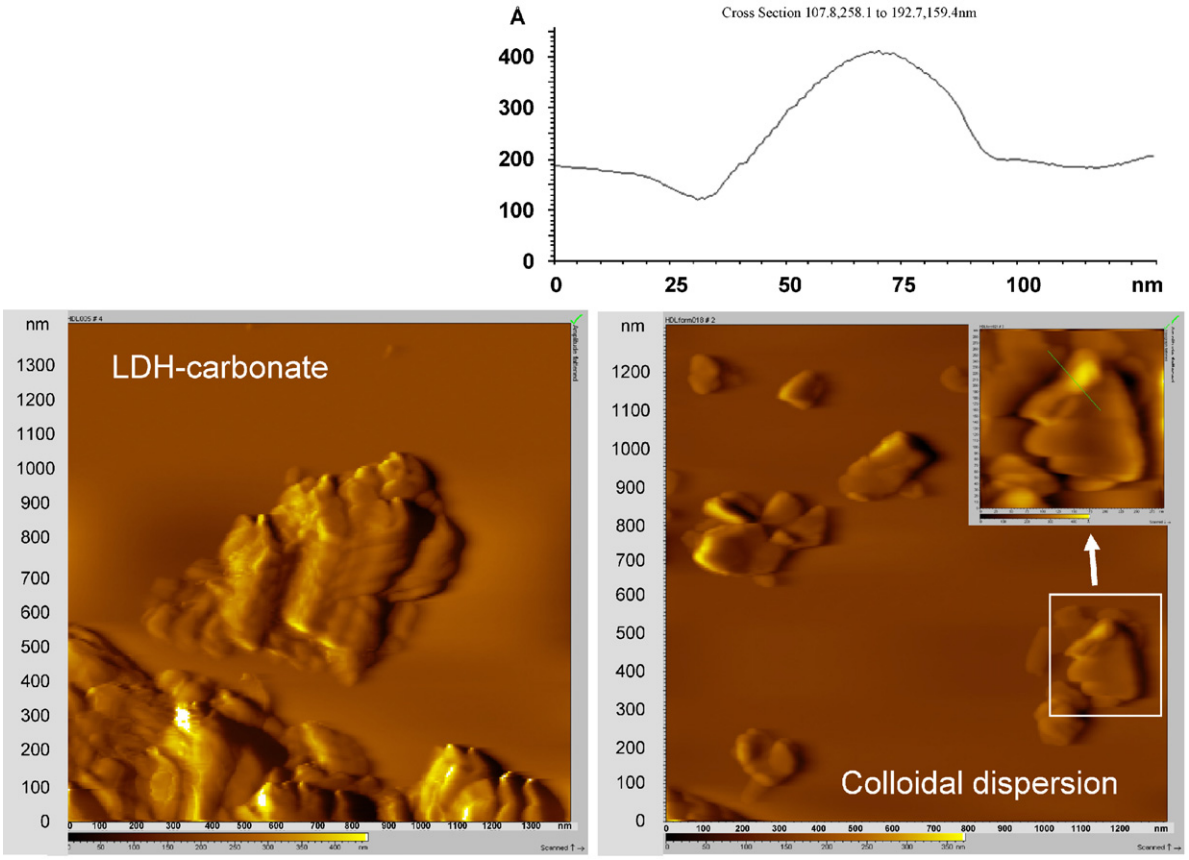

Fig. 6. AFM images: LDH-carbonate (amplitude; image scales: 1400 × 1400 nm); colloidal dispersion dropped on mica (amplitude; image scales: 1320 × 1320 nm). The small box at the superior right corner shows topographical image (image scales: about 290 × 290 nm). The height profile of a particle from the colloidal dispersion is also shown.

exhibits much smaller particles with dimensions that are comparable to those observed by TEM (medium size of approximately 190 nm × 230 nm). The exfoliation process probably breaks the pristine LDH-carbonate particles and/or it is preferential for small particles (if this was the case, the sediment composed by LDH-carbonate should contain the largest particles). The topographical image for a particle from colloidal dispersion shows a profile that is very similar to that observed from TEM image: sheet-like particles curled at the edges. The thickness of the curled edge is about 40 nm as estimated from the height profile (Fig. 6). Hence, the AFM images reveal that colloidal dispersion particles exhibit quite distinct dimensions and morphologies from pristine LDH-carbonate particles, supporting the proposed exfoliation process.

The results described above show that decarbonation and exfoliation of Hydrotalcite are promoted by a DMF–ethanol mixture. Attempts to explain the behavior of the LDH-carbonate in the presence of amide and alcohol required us to think about anionic species that could replace the carbonate anion in the LDH structure. It is well known that amides (R-CONR_2) can undergo solvolysis in base-catalyzed conditions [46]. A plausible hypothesis to be investigated, therefore, should be the generation of formate ions ($HCOO^-$) from DMF hydrolysis since LDH-carbonate is a hydrated solid able to promote base-catalyzed reactions [47]. Aiming to improve the characterization of the product obtained from the interaction between LDH-carbonate and the organic solvents, the LDH-formate material was synthesized. It should be mentioned that no previous report about preparation of LDH-formate was found in the literature.

3.2. LDH-formate material

Three different procedures were used trying to intercalate formate ions into the LDH layers: ion-exchange (from LDH-chloride), co-precipitation (from metal nitrate solutions at pH 10) and re-precipitation. Although, the first and second methods are the most used for intercalation of anionic species into LDH layers, attempts using formate were unsuccessful here. Results from XRD, FTIR and thermogravimetric analysis showed low amounts of $HCOO^-$ in the products. The re-precipitation method, however, allowed partial intercalation of the formate anions. The characterization of the product isolated by this procedure, LDH-formate, is discussed further on.

The Mg/Al experimental ratio (Mg/Al = 2.1) for LDH-formate is about one unity lower than that for starting LDH-carbonate (Mg/Al = 3.1). The significant difference

suggests that some magnesium ions could be lost during dissolution and re-precipitation processes. As expected, the XRD pattern (not shown) of LDH-formate is similar to that of the pristine LDH-carbonate since $HCOO^-$ and CO_3^{2-} anions are very similar in size. Assuming that the brucite-like layer thickness is 0.48 nm, the gallery height for LDH-formate should be very close to that of LDH-carbonate (about 0.3 nm). Thus, the data suggest a monolayer arrangement for the intercalated formate anion flat-oriented in the interlayer region.

3.3. Comparison of LDH-samples and LDH-formate by FTIR and FT-Raman

LDH-samples isolated from DMF–ethanol mixtures, as exemplified here for LDH-sample C, exhibited higher carbon contents than the pristine LDH-carbonate (see Section 2). This result is coherent with an exchange of carbonate (divalent ion) by formate (monovalent ion) species.

FTIR spectra of LDH-carbonate, LDH-formate, colloidal dispersion, LDH-sample C and LDH-sample A are shown in Fig. 7. Characteristic Hydrotalcite IR bands are observed for LDH-carbonate (see attributions in Section 2). LDH-formate spectrum shows a few differences compared to LDH-carbonate evidencing intercalation of formate anions. A very broad band at 3500–2500 cm^{-1} suggests that the water molecules are probably also hydrogen bonded to formate ions. The band at 1587 cm^{-1} can be ascribed to ν_a(COO) asymmetric stretching of formate groups [48]. The ν_s(COO) symmetric stretching that should be observed at about 1370 cm^{-1} maybe overlaps the CO_3^{2-} band at 1373 cm^{-1}. FTIR spectra of the colloidal dispersion and LDH-sample C are very similar to LDH-formate spectrum, except for the relative intensities of some bands. The presence of $HCOO^-$ ion in these materials is suggested by the appearance of a new band at 1584 cm^{-1} that can be ascribed to ν_a(COO) mode. For comparison, it is interesting to examine the spectrum of LDH-sample A (isolated from 100% DMF). It shows typical bands of LDH-carbonate in addition to other new bands. A weak band at 1590 cm^{-1} can be attributed to ν_a(COO) of the formate anion while the band at 1153 cm^{-1} (rock(CH_3) and/or ν(CNC)) [49] is characteristic of dimethylamine that could be adsorbed on LDH layers through hydrogen bonds with hydroxide groups. The presence of dimethylamine is coherent with the reaction proposed further on. The absorptions at about 1220 cm^{-1} could not be unambiguously ascribed (in this region one could expect vibrational bands of ethers, esters, alcohols or ketones, for example).

FT-Raman spectra of LDH-carbonate, LDH-formate, colloidal dispersion, LDH-sample C and sodium formate are shown in Fig. 8. LDH-formate, colloidal dispersion and LDH-sample C exhibit bands that are characteristic of the LDH host (550 cm^{-1}) [19] and carbonate ions ($\nu_1 = 1058\ cm^{-1}$) [48]. Since the absorption related to ν_3 carbonate stretching vibration is very weak in Raman spectrum [19,48], the region of 1400–1350 cm^{-1} can be analyzed without interference from this band. The bands at this region for LDH-formate, colloidal dispersion and LDH-sample C can, therefore, be ascribed to organic species. The similarity between the spectra of these three samples and sodium formate indicates that the formate organic guest is immobilized as anionic ($HCOO^-$) instead

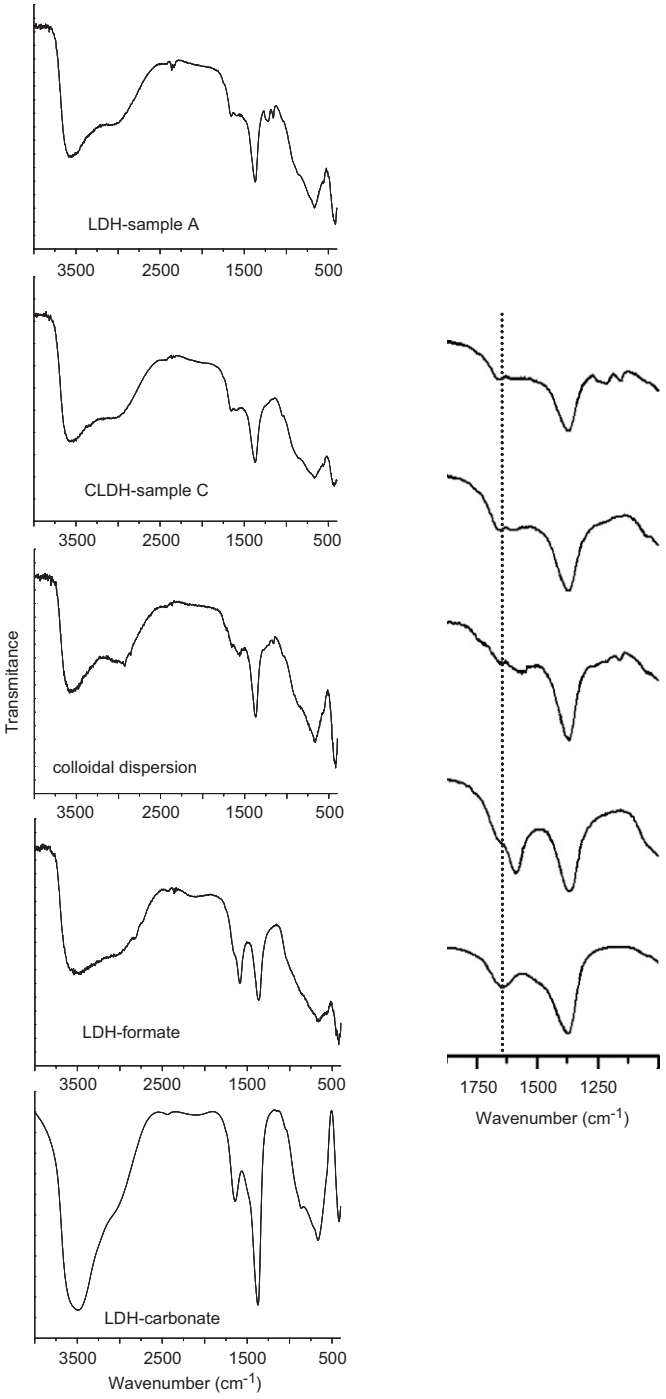

Fig. 7. FTIR spectra of LDH-carbonate, LDH-formate, colloidal dispersion, LDH-sample C and LDH-sample A at 4000–400 cm^{-1} (left). FTIR spectra of the same samples at 1875–1000 cm^{-1} (right).

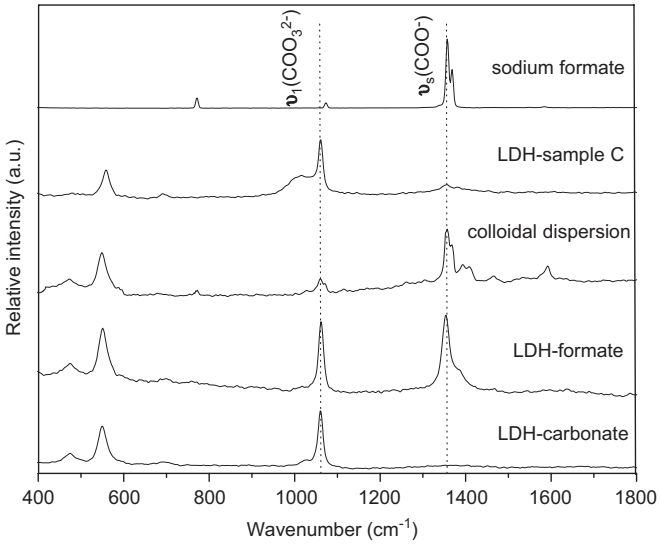

Fig. 8. FT-Raman spectra of LDH-carbonate, LDH-formate, colloidal dispersion, LDH-sample C and sodium formate. Laser line = 1064 nm.

of acidic form (HCOOH) on LDH. The v_{as} and v_s stretching vibrations of the LDH-formate $-COO^-$ group are observed, respectively, at 1587 cm^{-1} (data from FTIR) and 1351 cm^{-1} (data from FT-Raman). The Δv ($v_{as}-v_s$ = 236 cm^{-1}) value is close to that observed for the sodium salt of formate (data from IR: v_{as} = 1567, v_s = 1366 cm^{-1}; Δv = 201 cm^{-1} [48]). Thus, it is possible to state that formate anions are interacting as free ions with the LDH hydroxylated layers (i.e., the carboxylate group is not monodentate coordinated to the metal sites in the LDH layers). LDH-formate and colloidal dispersion, as well as LDH-sample C, do not show band at 1724 cm^{-1} that could be assigned to ν(C = O), indicating the non-existence of the acidic form of the organic guest in those samples. The absorptions for colloidal dispersion at 1393 cm^{-1} and 1409 cm^{-1} could be ascribed, respectively to $\delta_s(CH_3)$ and/or ν(N-CO), and $\delta_s(CH_3)$ modes of DMF [50], if it is assumed that some DMF molecules could be adsorbed on the LDH surfaces. The band at 1591 cm^{-1} can be attributed to $v_a(COO)$ of carboxylate group, as previously observed for ibuprofenate and acetate ions [19,51].

3.4. Proposed reactions for decarbonation and exfoliation of Hydrotalcite

In general, treatment of LDH-carbonate with weak inorganic or organic acids leads to the protonolysis of carbonate (CO_3^{2-}) anions producing CO_2 and water [42]. The control of the pH allows carbonate ions being exchanged by the conjugated base of the weak acid without solubilization of the hydroxide layer. This reaction is useful to prepare LDHs from LDH-carbonate by exchange method. The neutralizing and buffering properties of the LDH Mg,Al-CO_3^{2-} (a pharmaceutical antacid) are also related to protonolysis. The neutralization by HCl in this case involves the reaction between LDH intercalated-carbonate anions and H_3O^+ ions, followed by insertion of chloride ions into the layers. Then, the brucite-like layers react with HCl and the ions Mg^{2+} and Al^{3+} are released into the solution (the trivalent ion is leached following the divalent one) [52]. These data suggest that carbonate sites are stronger bases than brucite-like layer hydroxide groups in aqueous medium.

The studies carried out here revealed the presence of formate anions in the samples isolated during decarbonation and exfoliation of Hydrotalcite (i.e., colloidal dispersion and LDH-sample C). The formation of these carboxylate ions can be explained by assuming the hydrolysis of DMF. Since the LDH-carbonate exhibits basic character, the DMF is subjected to an alkaline medium. Under this basic condition, the amide ($HCON(CH_3)_2$) can undergo hydrolysis giving formate ($HCOO^-$) anion and dimethylamine ($HN(CH_3)_2$) as products [46]. The net reaction for this process is proposed in Scheme 1.

Mechanistic studies are out of the scope of this work since the pathways to carry out Hydrotalcite decarbonation are not straightforward. At a first glance, DMF hydrolysis could be achieved through reaction with basic sites of Hydrotalcite, i.e., brucite-like layer hydroxide groups, intercalated carbonate ions and/or intercalated (and superficial) water molecules. Although mechanisms for amide hydrolysis catalyzed by bases in bulk water have been explored in the literature [53], no studies were found about amide hydrolysis in heterogeneous hydrated systems like the one investigated here.

It is clear that the DMF is essential for Hydrotalcite decarbonation and exfoliation processes. It is also certain that ethanol enhances the DMF hydrolysis since the extension of the reaction is low in presence of the pure amide. It has also been observed in the literature [30] that LDH-carbonate submitted to ultrasonic treatment for about 600 min in pure formamide is not delaminated.

Although the presence of ethanol is important, the role of this second solvent is not understood. It is known that DMF-alcohol mixed solvent can exhibit several types of molecular complexes depending on the proportions of amide and alcohol in the mixture, as recently reported for DMF–methanol mixtures [54]. Additionally, according to theoretical calculations [46] for DMF hydrolysis, the amide itself and also the transition state of the tetrahedral intermediate ($HC(O^-)OH(N(CH_3)_2)$) must be solvated by water in the hydrolysis process. Thus, ethanol could be important for stabilization of molecular complexes probably involved in the hydrolysis reaction. On the other hand, the possibility of alcohol acting as a reactant cannot be completely ruled out since, in the presence of amides, ethanol can give ester that can be transformed into carboxylic acids. The number of species that could be intermediately formed in the DMF hydrolysis process maybe is responsible for a few FTIR and Raman bands that could not be unambiguously assigned in this work.

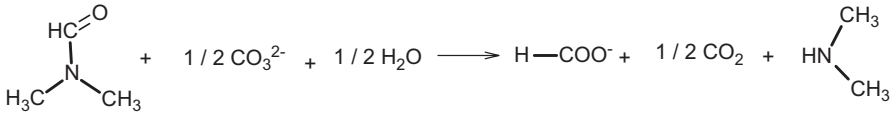

Scheme 1.

In previous reports, formamide ($HCCONH_2$) has been regarded as the best solvent to exfoliated LDHs. However, the role of this amide for delamination of LDHs has not yet been well elucidated until the moment. Furthermore, it was observed that LDH exfoliated layers gradually dissolve in formamide dispersion [13]. Taking into account the results of our work, it is plausible to infer that in the cases of exfoliation by formamide, the hydroxide layer could promote the amide hydrolysis giving formate/formic acid (and ammonia) and be slowly dissolved by an acid–base reaction. Starting from carbonate-containing LDH (a intercalated anion more basic than nitrate, chloride or perchorate ions), the amide could preferentially react with CO_3^{2-} giving CO_2, water and formate ion, endorsing the anion exchange reaction. As mentioned before, carbonate basic sites seem to be stronger than hydroxide groups from LDH layers. Once intercalated between the LDH layers, the $HCOO^-$ anions could promote the osmotic swelling process and the material exfoliation.

The data reported in the present work increases the number of methods to reach colloidal dispersions of exfoliated LDHs nanosheets. Future studies should investigate experimental conditions aiming to maximize the carbonate deintercalation by protonolysis reaction and also minimize the solubilization of brucite-like layers.

4. Conclusions

The behavior of Hydrotalcite in two different organic solvents, *N*,*N*-dimethylformamide and ethanol and also in mixtures of these solvents, has been investigated. It has been revealed that LDH-carbonate can directly undergo decarbonation and exfoliation in 1:1 (v/v) DMF–ethanol solvent mixture at ambient temperature. The process involves the hydrolysis of DMF promoted by basic centers of hydrated Hydrotalcite and, consequently, decomposition of carbonate in CO_2 (and H_2O). Formate ions are produced in the hydrolysis and intercalated into brucite-like layers. LDH-formate phase should be swelled in DMF–ethanol medium, promoting layers separation and the stabilization of a colloidal dispersion of nanosized LDH particles.

The study here reported provides an interesting method to prepare new intercalated LDH materials starting from the stable LDH-carbonate precursor. LDH-formate phase can be produced in situ and used as an intermediate for intercalation of robust and low-polar molecules since the monovalent formate anions are not strongly bounded to LDH and, therefore, the layers can be separated in high extension (exfoliation).

Acknowledgments

The authors acknowledge financial support and fellowships from the Brazilian agencies Fundação de Amparo à Pesquisa do Estado de São Paulo (FAPESP) and Conselho Nacional de Desenvolvimento Científico e Tecnológico (CNPq). We are also thankful to Dr. D.L.A. de Faria and R. Ando from Laboratório de Espectroscopia Molecular (Instituto de Química-USP) for Raman spectra; Dr. P.K. Kiyohara and S.P. Toledo from Instituto de Física-USP for SEM and TEM images recording; Dr. M.A. Bizeto for help with TEM data analysis; Dr. H.E. Toma and Ms. L.S. Bonifácio from the Instituto de Química-USP for AFM facility and valorous assistance. We also appreciate the support from the Instituto do Milênio de Materiais Complexos (IM^2C).

References

[1] A.J. Jacobson, in: G. Alberti, T. Bein (Eds.), Colloidal Dispersion of Compounds with Layer and Chain Structures, Comprehensive Supramolecular Chemistry, vol. 7, Pergamon, New York, 1996, p. 315.
[2] R. Tenne, Angew. Chem. Int. Ed. 42 (2003) 5124.
[3] E.T. Thostenson, C. Li, T.-W. Chou, Composites Sci. Technol. 65 (2005) 491.
[4] G. Alberti, S. Cavalaglio, C. Dionigi, F. Marmottini, Langmuir 16 (2000) 7663.
[5] W.M.R. Divigalpitiya, R.F. Frindt, S.R. Morrison, Science 246 (1989) 369.
[6] T. Sazaki, M. Watanabe, J. Am. Chem. Soc. 120 (1998) 4682.
[7] M.A. Bizeto, V.R.L. Constantino, Mater. Res. Bull. 39 (2004) 1811.
[8] M.I. Shukoor, H.A. Therese, L. Gorgishvili, G. Glasser, U. Kolb, W. Tremel, Chem. Mater. 18 (2006) 2144.
[9] F. Leroux, C. Taviot-Gueho, J. Mater. Chem. 15 (2005) 3628.
[10] F. Trifirò, A. Vaccari, in: G. Alberti, T. Bein (Eds.), Solid State Supramolecular Chemistry Two- and Three-Dimensional Inorganic Networks, vol. 7, Pergamon, New York, 1996, p. 251.
[11] F. Cavani, F. Trifirò, A. Vacari, Catal. Today 11 (1991) 173.
[12] B.F. Sels, D.E. deVos, P.A. Jacobs, Catal. Rev. 43 (2001) 443.
[13] K. Kaneda, K. Ebitani, T. Mizugaki, K. Mori, Bull. Chem. Soc. Jpn. 79 (2006) 981.
[14] C.A.S. Barbosa, P.M. Dias, A.M.C. Ferreira, V.R.L. Constantino, Appl. Clay Sci. 28 (2005) 147.
[15] F. Leroux, J.P. Besse, Chem. Mater. 13 (2001) 3507.
[16] M. Darder, M. Lopez-Blanco, P. Aranda, F. Leroux, E. Ruiz-Hitzky, Chem. Mater. 17 (2005) 1969.
[17] N.K. Lazaridis, A. Hourzemanoglou, K.A. Matis, Chemosphere 47 (2002) 319.
[18] C. Del Hoyo, Appl. Clay Sci. (2006), doi:10.1016/j.clay.2006.06.010.
[19] C.R. Gordijo, C.A.S. Barbosa, A.M.C. Ferreira, V.R.L. Constantino, D. de Oliveira Silva, J. Pharm. Sci. 94 (2005) 1135.
[20] M. Adachi-Pagano, C. Forano, J.P. Besse, Chem. Commun. (2000) 91.
[21] F. Leroux, M. Adachi-Pagano, M. Intissar, S. Chauvière, C. Forano, J.P. Besse, J. Mater. Chem. 11 (2001) 105.

[22] M. Singh, M.I. Ogden, G.M. Parkinson, C.E. Buckley, J. Connolly, J. Mater. Chem. 14 (2004) 871.
[23] J.T. Rajamathi, N. Ravishankar, M. Rajamathi, Solid State Sci. 7 (2005) 195.
[24] S. O' Leary, D. O'Hare, G. Seeley, Chem. Commun. (2002) 1506.
[25] Y. Guo, H. Zhang, L. Zhao, G.D. Li, J.S. Chen, L. Xu, J. Solid State Chem. 178 (2005) 1830.
[26] M. Jobbagy, A.E. Regazzoni, J. Colloid Interface Sci. 275 (2004) 345.
[27] B.R. Venugopal, C. Shivakumara, M. Rajamathi, J. Colloid Interface Sci. 294 (2006) 234.
[28] T. Hibino, W. Jones, J. Mater. Chem. 11 (2001) 1321.
[29] T. Hibino, Chem. Mater. 16 (2004) 5482.
[30] Q.L. Wu, A. Olafsen, O.B. Vistad, J. Roots, P. Norby, J. Mater. Chem. 15 (2005) 4695.
[31] L. Li, R.Z. Ma, Y. Ebina, N. Iyi, T. Sasaki, Chem. Mater. 17 (2005) 4386.
[32] Z.P. Liu, R.Z. Ma, M. Osada, N. Iyi, Y. Ebina, K. Takada, T. Sasaki, J. Am. Chem. Soc. 128 (2006) 4872.
[33] K. Okamoto, T. Sasaki, T. Fujita, N. Iyi, J. Mater. Chem. 16 (2006) 1608.
[34] R. Ma, Z. Liou, L. Li, N. Iyi, T. Sasaki, J. Mater. Chem. 16 (2006) 3809.
[35] T. Hibino, M. Kobayashi, J. Mater. Chem. 15 (2005) 653.
[36] C. Jaubertie, M.J. Holgado, M.S. San Roman, V. Rives, C, Chem. Mater. 18 (2006) 3114.
[37] W. Chen, L. Feng, B. Qu, Chem. Mater. 16 (2004) 368.
[38] L. Qiu, B. Qu, J. Colloid Interface Sci. 301 (2006) 347.
[39] B.R. Venugopal, N. Ravishankar, C.R. Perrey, C. Shivakumara, M. Rajamathi, J. Phys. Chem. B 110 (2006) 772.
[40] L. Li, R. Ma, N. Iyi, Y. Ebina, K. Takada, T. Sasaki, Chem. Commun. (2006) 3125.
[41] C.A.S. Barbosa, A.M.C. Ferreira, V.R.L. Constantino, A.C.V. Coelho, J. Incl. Phenom. Macrocyclic Chem. 42 (2002) 15.
[42] P.S. Braterman, Z.P. Xu, F. Yarberry, in: S.M. Auerback, K.A. Carrado, P.K. Dutta (Eds.), Handbook of Layered Materials, Marcel Dekker, New York, 2004, p. 373.
[43] J. Zhang, F. Zhang, L. Ren, G.D. Evans, X. Duan, Mater. Chem. Phys. 85 (2004) 204.
[44] JCPDS file 7-378.
[45] G.S. Thomas, P.V. Kamath, J. Chem. Sci. 118 (2006) 127.
[46] Y. Xiong, C.-G. Zhan, J. Phys. Chem. A 110 (2006) 12644.
[47] V.R.L. Constantino, T.J. Pinnavaia, Inorg. Chem 34 (1995) 883.
[48] K. Nakamoto, Infrared and Raman Spectra of Inorganic and Coordination Compounds, Part A: Theory and Applications in Inorganic Chemistry, fifth ed., Wiley, New York, 1997 (p. 59).
[49] G.A. Guirgis, S. Bell, C. Zheng, J.R. Durig, Phys. Chem. Chem. Phys. 4 (2002) 1438.
[50] P. Drozdzewski, A. Brozyna, M. Kubiak, J. Mol. Struct. 707 (2004) 131.
[51] D.C. Pereira, D.L.A. de Faria, V.R.L. Constantino, J. Braz. Chem. Soc. 17 (2006) 1651.
[52] Z. Kokot, Pharmazie 43 (1988) 249.
[53] D. Bakowies, P.A. Kollman, J. Am. Chem. Soc. 121 (1999) 5712.
[54] J. Stangret, E.K. Piotrowicz, J.S. Cybulska, Spectrochim. Acta Part A 61 (2005) 3043.